PHYSICAL PROPERTIES AND ENVIRONMENTAL PERFORMANCE OF STEAM-CURED CONCRETE CONTAINING FLUE-GAS DESULFURIZATION GYPSUM

Hongseok Jang[1] and Seungyoung So[2]*

ABSTRACT

Flue-gas desulfurization (FGD) gypsum has occasionally been used as an additive to cement. Consequently, appropriate facilities are required to ensure the environmentally safe processing of FGD gypsum and the resulting cement material properties. Such facilities are yet to be developed because the amount of FGD gypsum used is still small when compared with the vast amounts of FGD gypsum generated. In this study, we analyze the effect of FGD gypsum addition on the physical properties, stabilization, and radon count of steam-cured mortar and compare its performance with air-cured mortar. Our results show that the steam-cured pozzolanic hydration products of ettringite and C-S-H promote the densification of the mortar structure, thereby resulting in nanopore size reduction and increased strength of FGD gypsum mortar subsequent to the steam-cured hydration process. Further, our environmental test results indicate that steam-cured pozzolanic materials composed of FGD gypsum are environmentally safer than air-cured cementitious materials.

KEYWORDS

FGD gypsum, nanopores, leaching toxicity, recycled material

INTRODUCTION

FGD gypsum is a major byproduct generated from coal-burning thermal power plants. In general, FGD byproducts consist of substances whose compositions vary according to the desulfurization processes utilized in the plant; this makes the continuous monitoring of these byproducts and ensuring of human safety necessary. In the context of current concerns regarding the environmental friendliness and safety of coal-combusted materials and atmospheric air quality, the degree of regulation of coal-burning thermal plants is expected to become increasingly stringent.

Over the past few decades, most coal-burning thermal power plants have been equipped with FGD facilities to comply with regulations and laws established to control atmospheric emissions of SO_2 (Council Directive 1988, 1994, 2001). Diverse kinds of FGD processes are currently in use, with the wet limestone FGD process forming the pre-dominant choice

1.Ph.D., Joenbuk National University, Department of Architectural Engineering, Korea.
2.* Ph.D., Professor, Joenbuk National University, Department of Architectural Engineering, Research Center of Industrial Technology, Korea, e-mail: archiso@jbnu.ac.kr (Corresponding Author).

corresponding to ~80% of the market share (Lvarez-Ayuso et al. 2008). SO_2 gas, which is an exhaust gas in flue, is removed through its adsorption by limestone slurry, which is further oxidized to form a sulfate. The sulfate is extracted as gypsum slurry, which is eventually dehydrated, leaving behind the so-called FGD gypsum (Lvarez-Ayuso et al. 2008). Meanwhile, concurrent with intensifying environmental regulations, FGD gypsum production is also expected to increase; Annual production amount of FGD gypsum in Korea approximates four million tonnes; and other countries, also producing these residues, try to find safe solutions for the their reuse. This will require the framing and implementation of suitable environmental safety measures for such materials.

In general, gypsum is used as an essential element to improve the properties of cement concrete. Gypsum activates the pozzolanic reaction, and thus, it can be used in preparing high-strength concrete. However, in Korea, there are no mines yielding natural gypsum; the country is fully dependent on imports of natural gypsum. In addition, crushing and classification processes are required to use general gypsum as a raw material for cement concrete, for which high energy consumption is unavoidable. Accordingly, researchers have suggested the use of FGD gypsum instead of general gypsum. FGD gypsum has occasionally been used as an additive to cement. Consequently, appropriate facilities are required to ensure the environmentally safe processing and physical properties of the resulting cement material. Such facilities are still to be developed because the amount of FGD gypsum used is very small relative to the amount of generated. Even so, researchers have already explored and utilized several methods to apply FGD gypsum in the field of agriculture (Clark et al. 2001). FGD gypsum is highly alkaline, and therefore, it has been employed in conditioning acid soils or providing essential nutrients such as sulfur for plant growth. However, the application of FGD gypsum to soils requires the appropriate assessment and pretreatment of pollutants such as heavy metals that may be present. Direct landfilling with FGD gypsum without the necessary treatment requires vast reclamation areas, which leads to wastage of land and soil and the risk of secondary pollution of the natural environment (Wang et al. 2016).

Thus, the environmental issues involved in the reuse of desulfurized gypsum must be appraised. Against this backdrop, in this study, we prepared "FGD gypsum mortar" with diverse mixing ratios and considered the curing conditions to evaluate the resulting physical properties. In particular, our efforts were concentrated on the possibility of ensuring stable recycling of FGD gypsum by evaluating the degree of radon emission and fixation of heavy metals after the curing of cement mortars.

MATERIALS

In the present study, we used ordinary Portland cement (OPC), which conforms to requirements specified in the Korean Standard KS L 5201 (Korea standard 2016). Ground granulated blast-furnace slag (GGBS), collected from a "K" steel plant in Korea, was used as the pozzolanic material. The GGBS specific area and specific weight were approximately 4200 cm^2/g and 2.91 g/cm^3, respectively.

FGD gypsum was acquired from a domestic coal-burning thermal power plant. The samples used in the present study were collected from three places in the power plant, mixed together, and homogenized to obtain "unified" ones before they were disposed for reclamation. Table 1 summarizes the results of our X-ray fluorescence (XRF) analysis of FGD gypsum and natural gypsum, both of which are composed primarily of CaO and SO_3.

TABLE 1. Chemical composition of raw materials.

Sample	Chemical Composition (%)						Specific gravity
	SiO_2	CaO	Al_2O_3	Fe_2O_3	MgO	SO_3	
OPC	21.74	61.06	5.86	3.22	3.99	2.43	3.15
FGD Gypsum	3.11	68.9	1.37	0.58	1.14	23.7	2.66
Natural gypsum	0.63	43.0	0.28	0.08	0.04	55.8	2.42
GGBS	34.76	41.71	15.02	0.48	6.87	0.13	2.91

EXPERIMENTAL DESIGN

Mix Proportion of Mortar Samples

FGD gypsum was mixed with GGBS and OPC according to a predetermined mixing ratio to produce cement mortar. For the present study intended to estimate the optimal mixing ratio of cement material consisting of FGD gypsum and GGBS, we prepared 10 batches of samples (Table 2). In particular, the composition of all batches was designed such that the ratio of GGBS and FGD gypsum was less than 0.4 times the ratio of the entire binder.

Curing Method

When steam is produced at atmospheric pressure at temperatures below 100 °C, this vapor forms a saturated atmosphere that can be utilized for special moisture curing. The general optimum temperature for curing has been estimated to lie in the range of (65–85)°C (Hanson 1997, Turkel et al. 2005). In this study, steam curing was conducted in accordance with ACI 517.2R-82

TABLE 2. Proportions of cementitious materials (%).

Type	OPC	GGBS	FGD gypsum
OGF0	100	—	—
OGF1	87	10	3
OGF2	85	10	5
OGF3	83	10	7
OGF4	77	20	3
OGF5	75	20	5
OGF6	73	20	7
OGF7	67	30	3
OGF8	65	30	5
OGF9	63	30	7

Mechanical Tests

The workability of the mortar was analyzed via flow table testing in accordance with the KS L 5105 and KS L 5111 standards (Korea standard 2017). Compressive strength tests for hardened mortars of the cementitious material were applied according to KS L 5105 (Korea standard 2007).

The particle size distribution and pore size were determined with the use of UPA-150 size distribution analyzers and a BELSORP mercury intrusion porosimeter, respectively. Scanning electron microscopy (SEM) observations were carried out with use of a JSM-5900 SEM. Thermogravimetric differential thermal analysis (TG-DTA) analysis was conducted with the use of a TA Q20 comprehensive thermal analyzer, and Fourier transform infrared spectroscopy (FT-IR) analysis was conducted using a JASCO 6300FV + IRT5000 instrument.

The leaching test of the prepared cement mortar specimens was carried out according to standard procedures specified in the US EPA Toxicity Characteristic Leaching Procedure Test (TCLP, EPA 1992). The heavy-metal concentration was analyzed via plasma emission spectrometry conducted with the Shimadzu ICPS 7500 OPTIMA. In particular, the mercury content was analyzed with the use of the Shimadzu AA-6200 instrument according to the procedure. The radon detector Durridge RAD7 was used for the radon tests (load factor 1.0 m^2/m^3). Here, we note that the RAD7 continuous monitor (Durridge Company, USA) uses the static electricity collection of the alpha analyzer together with spectrum analysis to measure the radon concentration; this equipment is appraised and approved by US Environmental Protection Agency.

RESULTS AND DISCUSSION

SEM Image

Figure 1 presents the SEM image of FGD gypsum composed of gypsum crystals, which appear mostly ellipsoidal. Table 1 presents the results of our XRF analyses of FGD gypsum, natural gypsum, OPC and GGBS. CaO and SO_3 can be identified as the major chemical components of FGD gypsum. CaO possibly originates from limestone or the slurry containing $CaCO_3$ or CaO. Further, we note here that several gases containing sulfur were adsorbed in the high-temperature

FIGURE 1. SEM image of FGD gypsum.

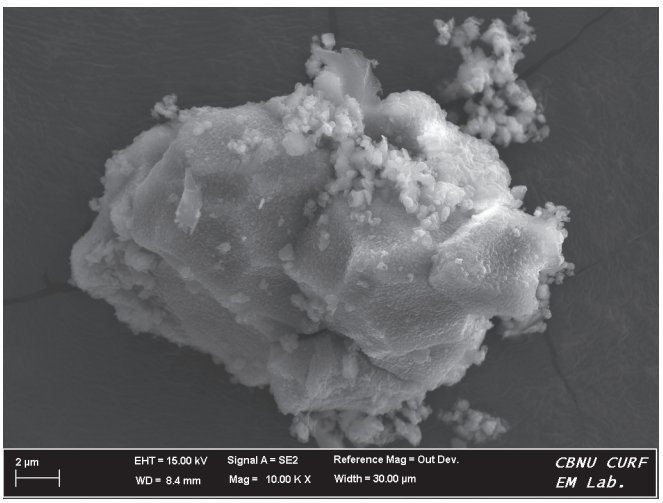

burner (Chen et al. 2014), which is why FGD gypsum contained a large amount of sulfur. GGBS and OPC, the ordinary binders, are broadly used as concrete mixtures, and in our study, they both exhibited an abundance of CaO.

Particle Size

As shown in Figure 2, we note that ~80% of the FGD gypsum particle size lies in the range from 0.01–0.1 mm with an average diameter of 0.04 mm. We note here that the particle size of uncrushed FGD gypsum is smaller than that of OPC. A smaller particle size can facilitate reactions between key components of gypsum and cement materials. In particular, FGD gypsum requires lower crushing energy than natural gypsum (Clark et al. 2001).

FIGURE 2. Particle size of materials: (a) FGD gypsum and (b) OPC.

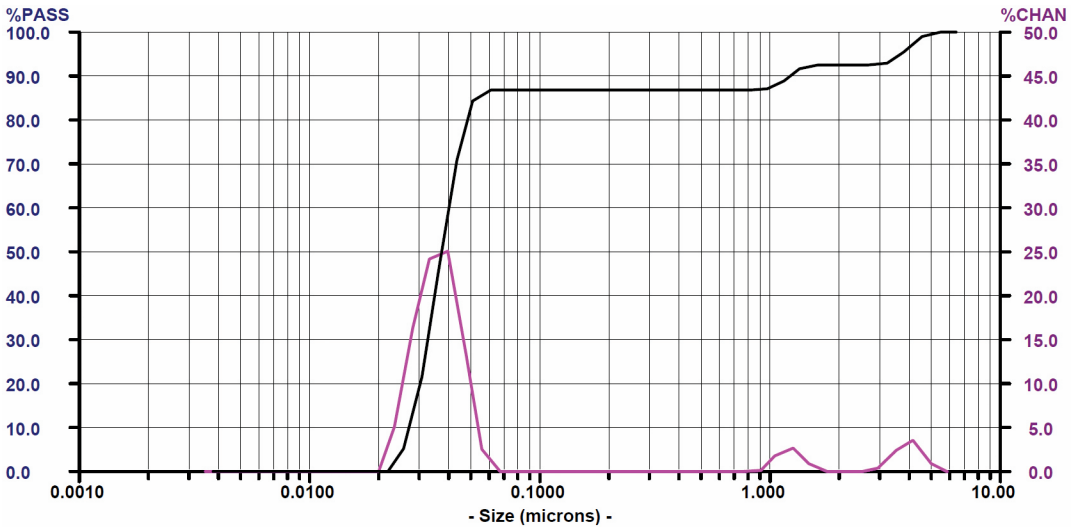

(a) FGD gypsum

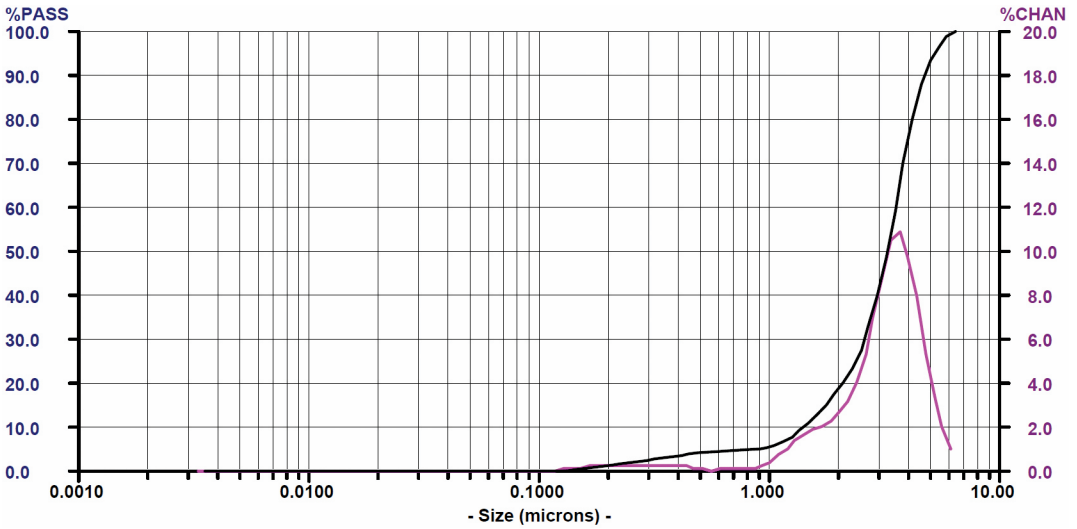

(b) OPC

TG-DTA Tests

The following equations describe the decomposition chemistry of wet-limestone FGD solids and the typical decomposition temperature ranges are also displayed (Buecker et al. 2004).

$$CaSO_4 \cdot 2H_2O \rightarrow CaSO_4 + 2H_2O\uparrow \ ((160–200)\ ^\circ C) \quad (1)$$

$$(CaSO_3 \cdot CaSO_4) \cdot \tfrac{1}{2}H_2O \rightarrow CaSO_3 \cdot CaSO_4 + \tfrac{1}{2}H_2O\uparrow \ ((400–450)\ ^\circ C) \quad (2)$$

$$CaCO_3 \rightarrow CaO + CO_2\uparrow \ ((650–800)\ ^\circ C) \quad (3)$$

Figure 3 shows the TG-DTA diagram for dried FGD gypsum. The mass loss of 0.16% at the first stage is related to the evaporation of chemically bonded water (Zhang et al. 2016). The second stage with a mass loss of 5.18% corresponds to the temperature range of 400–450 °C, relating to the release of water attributable to the decomposition of calcium sulfite semi-hydrate (Zhang et al. 2016). Finally, in the temperature range of 650–800 °C, the carbonate of calcium is decomposed, and CO_2 is released from FGD gypsum (Buecker et al. 2004).

Compressive Strength

Table 3 lists the compressive strengths of each type of FGD gypsum plus GGBS specimens used in the present study. The highest compressive strength corresponds to air-cured specimen OGF7 composed of 30% GGBS and 3% FGD gypsum. From the table, we note that the strength of

FIGURE 3. TG-DTA results of FGD gypsum.

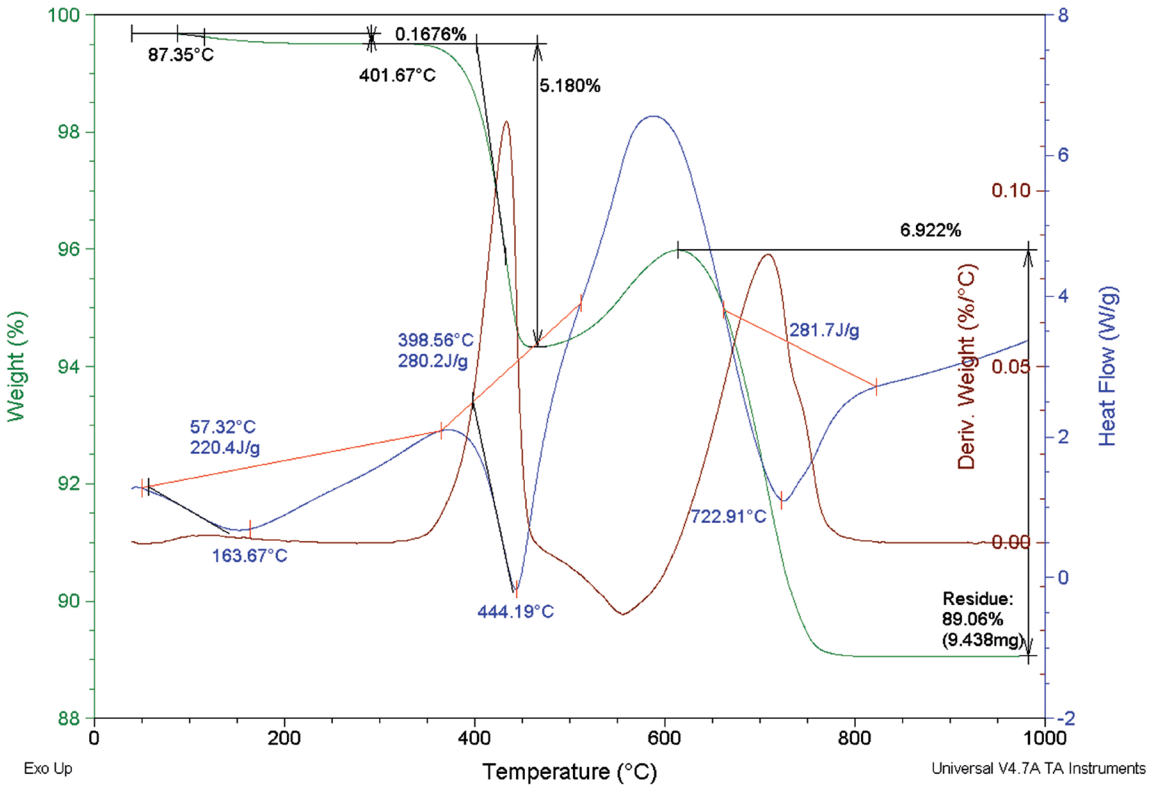

OGF7 increased by approximately 29.6% (7-days) and by 29.5% (28-days) relative to that of OPC mortar.

Here, we note that the addition of a tiny amount of FGD gypsum can disturb the complete transformation of the pozzolanic materials of Ca^{2+} and Al^{3+} ions contained in GGBS into ettringite due to lack of SO_3^{2-} ions (Mun 2002). The remaining Ca^{2+} and Al^{3+} ions react with water forming C_4AH_{13} or react with SO_3^{2-} ions contained in the ettringite (Mun 2002). Consequently, they are transformed into monosulfate, which has been identified as having lower strength than ettringite (Mun 2002, Carbonell et al. 2002). On the other hand, the admixture of a large quantity of gypsum creates volumetric expansive pressure via transformation into ettringite thereby leading to the formation of cracks in mortar or deterioration of the bond strength of coagulated hydrates (Mun et al. 2003, Emin et al. 1993).

Thus, estimating the appropriate gypsum content is crucial for improving the compressive strength of mortar. In the present study, we found the combination of 30% of GGBS and 3% of FGD gypsum to be the optimal ratio leading to the most efficient pozzolanic reaction of GGBS. In our study, the steam-cured mortar compressive strength was higher by 2–34% (7 d or 28 d) than that of air-cured ones. In particular, the highest compressive strength was obtained from specimen OGF5 composed of 20% GGBS and 5% FGD gypsum. In the process of the steam curing of concrete, the hydration of cement progresses quickly, thereby accelerating the formation speed of ettringite and C-S-H that wraps around cement particles (Baoju et al. 2001). That is, the steam-curing process intensifies the pozzolanic reaction, and the physical properties of concrete vary according to varying amounts of pozzolanic materials and activating agents.

Hydration Products and FT-IR Analysis

Inorganic bonding materials (GGBS, fly ash, silica fume) are often used to replace OPC in the solidification or stabilization of inorganic industrial waste (Martin et al. 2016). Gypsum

TABLE 3. Proportions of cementitious materials (%).

Type	Flow value	Air-cured Compressive strength (MPa)			Steam-cured Compressive strength (MPa)		
		1 day	7 days	28 days	1 day	7 day	28 days
OGF0	14.9	4.82	17.05	20.59	14.21	17.12	21.50
OGF1	15.2	5.20	17.62	21.64	13.72	17.72	23.50
OGF2	15.4	4.91	17.13	22.52	14.54	19.09	23.91
OGF3	15.5	4.73	17.84	24.58	15.17	22.38	24.83
OGF4	15.8	5.35	18.70	21.83	14.74	19.87	22.23
OGF5	15.5	5.38	19.68	23.40	15.68	21.95	31.40
OGF6	15.2	5.70	18.86	21.72	16.15	21.40	27.15
OGF7	16.0	5.02	22.09	26.66	15.37	21.93	27.20
OGF8	15.7	5.22	20.42	22.81	16.15	21.56	25.09
OGF9	15.4	5.15	18.82	22.25	16.54	21.17	26.34

increases the compressive strength relative to the no-gypsum. As the glassy film of GGBS is destroyed by the stimulation of sulfate, various ions eluted from GGBS react with gypsum to make ettringite and gradually form C-S-H (Mun et al. 2003). This means that the gypsum not only acts as a stimulant to destroy the film but also reacts with GGBS to act as a binder (Mun 2002, Mun et al. 2003).

In general, FT-IR spectrometry is used to measure the vibration, rotation, and stretching of molecular frameworks. Figure 4 presents the FT-IR spectra result of the OGF5 mortar cured in air or by steam. Both sets of spectra show peaks at (3640, 3440, 1630, 1440, 1100, 1000, and 875) cm^{-1}. These peaks indicate that both specimens have the crystal structure of ettringite or C-S-H. Further, the overall peaks in the spectra of the specimen cured by steam tend to exhibit reduced intensities relative to the other spectra. The peak at 3640 cm^{-1} is attributed to the stretching vibration of O–H ions (Robert et al. 1999). This band is related to Ca–OH stretching vibration in $Ca(OH)_2$ of ettringite (Zhang et al. 2011). The bands at approximately 3440 and 1630 cm^{-1} signify bending vibration of H–O–H water molecules (Mollah et al. 2000, Rikard et al., 2009). The peak at 875 cm^{-1} also denotes the bending vibration of Al–O–H (Robert et al. 1999).

The band at approximately 1440 cm^{-1} signifies the antisymmetric tensile vibration of CO_3 generated from reactions between carbon dioxide in the atmosphere and calcium hydroxide. In addition, the peak at 1100 cm^{-1} corresponds to the SO_4 component of ettringite (Peyvandi et al., 2015). Further, the band at 1000 cm^{-1} represents the presence of polymerized silicate. The strong and sharp peak in the vicinity of 1000 cm^{-1} observed in the present study was interpreted as the formation of a larger amount of C-S-H and increased hydration. In addition, the steam-cured mortar was concluded to have more water content than the mortar cured in air. That is, such peaks, associated with C-S-H and ettringite, tend to become more distinctive; this signifies the increase in the amounts of C-S-H and ettringite formed, and the C-S-H and ettringite are crystalized as they undergo hydration process.

FIGURE 4. FT-IR spectra of OGF5 mortar cured in air and steam for 28 days.

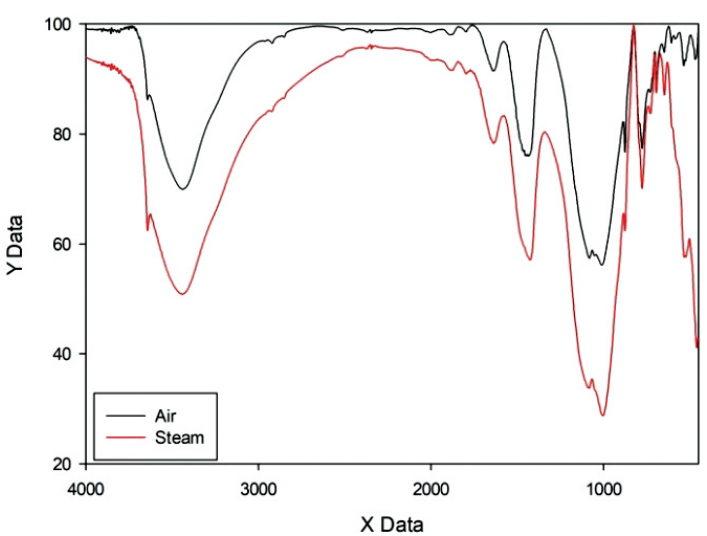

Environmental Friendliness

Cement materials developed with the use of steam-cured FGD gypsum can be exploited as construction materials, stabilizers, or coagulants, which necessitates their environmental impact assessments (Zhang et al., 2016). In the present study, we tested the FGD gypsum cement leaching toxicity and radon emission to determine the environmental friendliness of the prepared cement materials. Here, we note that the major issues related to the use of cement materials containing industrial wastes typically include the infiltration of certain toxic agents into groundwater (Turkel 2006, Yao et al. 2012).

Table 4 lists the results of the leaching test of FGD gypsum and other original specimens. The leaching of the original specimen of FGD gypsum results in a high concentration of Pb (0.4986 mg/ℓ), Cu (0.3571 mg/ℓ), As (0.7485 mg/ℓ), and low concentration of Cd (0.0537 mg/ℓ). These values still satisfy the criteria specified by the EPA (EPA 1992). Table 4 also presents the comparative results of the leaching test of heavy metals of the mixture to which 5% desulfurized gypsum was added. The OGF5 mortar prepared using FGD gypsum and GBFS exhibits Pb concentrations of 0.0150 mg/ℓ (air curing) and 0.0144 mg/ℓ (steam curing) and as concentrations of 0.253 mg/ℓ (air curing) and 0.0211 mg/ℓ (steam curing), whereas Cd and Cu are not detectable. On the contrary, from the mortar based on simple cement mixed with 5% of FGD gypsum, the amount of leaching appears to be higher than that of OGF5 mortar and affords slightly unsatisfactory results with respect to the fixation of As^{2+} and Cd^{2+} ions of FGD.

Our results indicate that the OGF5 specimen with higher compressive strength and improved physical properties exhibited greater reduction in the leaching of Pb, Cu, As, and Cd than the cement mortar simply mixed with FGD gypsum. In particular, the concentration of heavy metals leached from the steam-cured OGF5 specimen was lower than that leached from the OGF5 specimen cured in air. That is, the steam-cured cement mortar mixed with GBFS afforded the most effective reduction in the leaching of heavy metals from FGD gypsum.

TABLE 4. Leaching toxicity test results (mg/l).

Type	Condition	Pb	Cu	As	Cd	Hg
EPA Standard	—	5	50	5.0	1.0	0.2
OPC	Raw	0.076088	0.026544	0.032563	N.D.	N.D.
GGBS	Raw	0.058045	0.020862	0.003596	N.D.	N.D.
FGD Gypsum	Raw	0.49859	0.357132	0.748503	0.053716	N.D.
OPC mortar	Air-cured	0.009844	N.D.	0.008918	N.D.	N.D.
	Steam-cured	0.011482	N.D.	0.02405	N.D.	N.D.
5% FGD mortar	Air-cured	0.495342	0.354661	0.745781	0.06716	N.D.
	Steam-cured	0.488317	0.343578	0.749694	0.067921	N.D.
OGF5 mortar	Air-cured	0.015042	N.D.	0.025314	N.D.	N.D.
	Steam-cured	0.014429	N.D.	0.021135	N.D.	N.D.

*N.D.: Not detected

FIGURE 5. Nanopore size of OGF5 mortar cured in air and steam for 28 days.

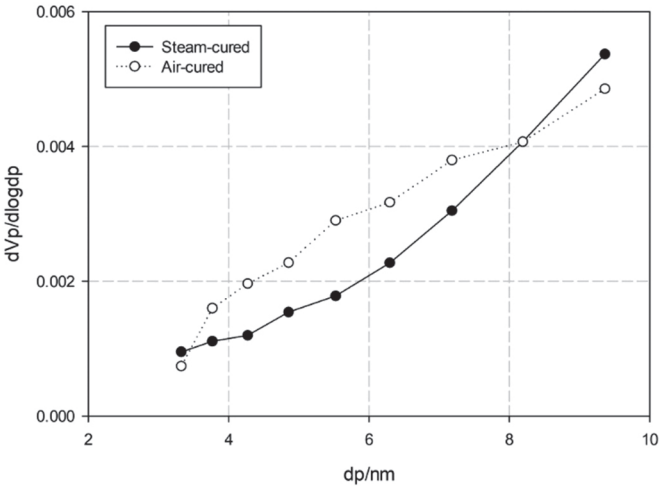

Here, we note that the concentrations of leached heavy metals presented in Table 4 lie within the limits specified in the Test Standards for Treatment of Wastes (CFR 2012). According our test results, the curing process of steam-cured cement mortar was found more effective than air curing with regard to the reduction in leaching of heavy metals from FGD gypsum.

The steam curing of cement mortar can improve the microporous structure of cement concrete by intensifying the pozzolanic reaction (Berry et al. 1990). Upon comparing the pozzolanic reaction of steam-cured OGF5 with that of an identical OGF5 specimen cured in air (see Figure 5), we can clearly observe the structural improvement evidenced by the smaller nanosized pores in the OGF5 specimen cured with steam. In this case, the hydrates are linked with the low porous compressive structure robustly connected to the cement matrix (see Figure 6(b)). In this regard, Na Zhang et al. (Zhang et al. 2016) have demonstrated that rod-shaped ettringite and C-S-H promote the densification of the mortar structure as a prominent hydrate and that they play a role in enhancing the compressive strength of pozzolanic material in the hydration process of steam curing.

FIGURE 6. Microstructure of OGF5 mortar cured in (a) air and (b) steam for 28 days.

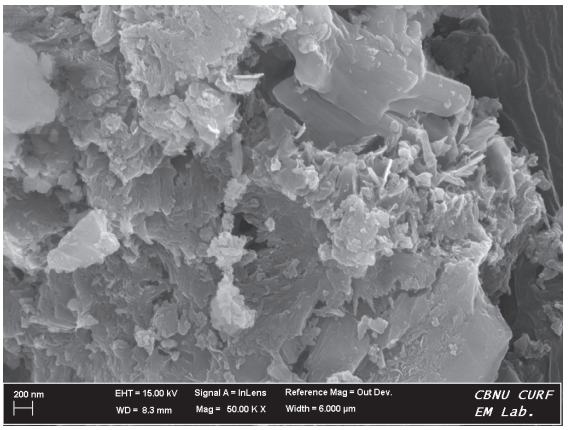

(a) OGF5—Air-cured

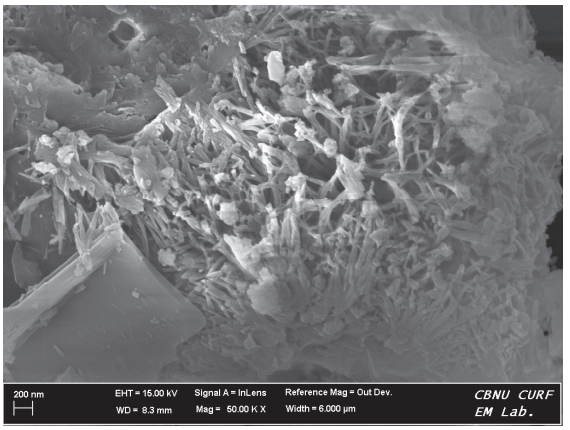

(b) OGF5—Steam-cured

TABLE 5. Radon emission of mortar (Bq/m^3).

	OPC		OGF5	
Type	Air-cured	Steam-cured	Air-cured	Steam-cured
Radon	55.5	57.35	87.32	81.03

Here, we remark that the annual production amount of FGD gypsum in Korea is nearly four million tons (ME 2014). Meanwhile, other countries are also producing these residues in their attempts to find safe solutions for FGD material reuse. One of the available applications of this byproduct is to employ gypsum as a constructional material. However, minerals such as gypsum necessarily need a preliminary assessment to determine the presence of any radioactive content and the radon emission degree (Campos et al. 2017).

From Table 5, we note that the exposure index of cement material composed of OGF5 cement mortar is less than 100 Bq/m^3. Thus, OGF5 as a construction material satisfies the emission requirements mandated by WHO (WHO 2009). The result indicates cement products based on FGD gypsum and pozzolanic materials cured with steam are environmentally acceptable.

CONCLUSION

In this research, we comprehensively investigated the material characteristics of steam-cured FGD gypsum mortar. The effects of FGD gypsum on the performance of steam-cured based cement binder were evaluated. Based on our abovementioned results, we draw the following conclusions:

- Untreated FGD gypsum contains high concentrations of Pb (0.4986 mg/ℓ), Cu (0.3571 mg/ℓ), As (0.7485 mg/ℓ), Cd (0.0537 mg/ℓ), and Hg (not detected). Without any reuse or treatment, the removal and dumping of FGD gypsum can lead to the wastage of valuable land resources.
- Various ions eluted from the pozzolanic material react with FGD gypsum and gradually form C-S-H gel. The resulting product plays a role in increasing the mechanical strength and can fix a greater amount of heavy metals.
- The radon exposure indices of OGF5 mortar are less than 100 Bq/m^3, which satisfies the WHO requirement.

ACKNOWLEDGEMENTS

This research was supported by the Basic Science Research Program under the aegis of the National Research Foundation of Korea (NRF) funded by the Ministry of Science, ICT & Future Planning (NRF-2018R1C1B6006462)

REFERENCES

ACI 517.2R-87 (1992), "Accelerated curing of concrete at atmospheric pressure-state of the art" *ACI manual of concrete practice part 5 : masonry, precast concrete, special processes*, pp.17.

Baoju L., Youjun X., Shiqiong Z. and Jian L. (2001). "Some factors affecting early compressive strength of steam-curing concrete with ultrafine fly ash" *Cement and Concrete Research* 31, 1455–1458.
Berry E. E., Hemmings R. T. and Cornelius B. J. (1990). "Mechanisms of hydration reactions in high volume fly ash pastes and mortars" *Cement and Concrete Composite* 12, 253–261.
Buecker B. and Blaine R. (2004). "Thermogravimetry: A great tool for flue gas desulfurization solids analysis" TA318 Instruments 1–6.
Campos M. P., Costa L. J. P., Nisti M. B. and Mazzilli B. P. (2017). "Phosphogypsum recycling in the building materials industry: assessment of the radon exhalation rate" *Journal of Environmental Radioactivity* 172, 232–236.
Carbonell-Barrachina A., DeLaune R. D. and Jugsujinda A. (2002). "Phosphogypsum chemistry under highly anoxic conditions" *Waste Manage* 22(6), 657–665.
Chen Z. W., Wu S. P., Li F. Z., Chen J. Y., Qin Z. H. and Pang L. (2014). "Recycling of flue gas desulfurization residues in gneiss based hot mix asphalt: Materials characterization and performances evaluation" *Construction and Building Materials* 73, 137–144.
Clark R. B., Ritchey K. D. and Baligar V. C. (2001). "Benefits and constraints for use of FGD products on agricultural land" *Fuel* 80(6), 821–828.
Council Directive 88/609/EEC of 24 November 1988 on the limitation of emissions of certain pollutants into the air from large combustion plants.
Council Directive 94/66/EC of 15 December 1994 amending Directive 88/609/EEC on the limitation of emissions of certain pollutants into the air from large combustion plants.
Directive 2001/80/EC of the European Parliament and of the Council of 23 October 2001 on the limitation of emissions of certain pollutants into the air from large combustion plants.
Emin E. and Halis O. (1993). "The mechanical properties of supersulphated cement containing phosphogypsum" *Cement and Concrete Research* 23(1), 115–121.
Hanson J. A. (1997). "Optimum steam curing procedure in precasting plants" *ACI Journal* 60(1), 75–100.
Jang H. S., Jeon S. H., So H. S. and So S. Y. (2014). "A study of the possibility of using TFT-LCD waste glass as an admixture for steam-cured PHC piles" *Magazine of Concrete Research* 66(4), 196–208.
Korea Standard association, KS L 5105 (2007). "Testing method for compressive strength of hydraulic cement mortar."
Korea standard association, KS L 5111 (2017). "Flow table for use in tests of hydraulic cement."
Korean Standard association, KS L 5201 (2016). "Portland cement."
Lvarez-Ayuso E. Á, Querol X. and Tomás A. (2008). "Implications of moisture content determination in the environmental characterisation of FGD gypsum for its disposal in landfills" *Journal of Hazardous Materials* 153, 544–550.
Maximum Concentration of Contaminants for Toxicity Characteristic, Protection of Environment 27, Chapter I—Environmental Protection Agency, Part 261—Identification and listing of Hazardous waste, Code of Federal Regulations (CFR) 40 CFR §261.24 (2012).
Mollah M. Y. A., Yu W., Schennach R. and Cocke D. L. (2000). "Fourier transform infrared spectroscopic investigation of the early hydration of Portland cement and the influence of sodium lignosulfonate" *Cement and Concrete Research* 30(2), 267–273.
Mun K. J. (2002). "Properties of non-sintered cement and concrete recycled with industrial waste" Ph.D. Thesis. Chonbuk National University 63–77.
Mun K. J., An Y. J., Yoon S. J. and Soh Y. S. (2003). "Utilization of waste phosphogypsum for concrete products cured by steam" In: Proceedings of Architectural Institute of Korea. Pusan, Korea: Pukyong National University, 359–362.
Peyvandi A., Holmes D., Soroushian P. and Balachandra A. M. (2015). "Monitoring of sulfate attack in concrete by ^{27}Al and ^{29}Si MAS NMR spectroscopy" *Journal of Materials in Civil Engineering* 27(8), 1–10.
Robert B. P. and Carl D. P. (1999). "Solubility of ettringite ($Ca_6[Al(OH)_6]_2(SO4)_3{\cdot}26H_2O$) at 5–75° C" *Geochimica et Cosmochimica Acta* 63(13), 1969–1980.
Study in management of industrial waste for alternative resource of natural materials (Desulfurization gypsum, waste lime, red mud), Resource Recirculation Research Division National Institute of Environmental Research Korea, NIER-RP2014-275 (2014).

Turkel S. (2006). "Long-term compressive strength and some other properties of controlled low strength materials made with pozzolanic cement and Class C fly ash" *Journal of Hazardous Materials* 137, 261–266.
Turkel S. and Alabas V. (2005). "The effect of excessive steam curing on Portland composite cement concrete" *Cement and Concrete Research* 35(2), 405–411.
US EPA Toxicity Characteristic Leaching Procedure, part of Test Methods for Evaluating Solid Waste, SW-846, Method 1311, US Environmental Protection Agency, Washington, DC, (1992).
Vyšvaril M. and Bayer P. (2016). "Immobilization of heavy metals in natural zeolite-blended cement pastes" *Procedia Engineering* 151, 162–169.
Wang J., Chen Q., Li Y., Zhuo Y. Q. and Xu L. Z. (2016). "Research on saline-alkali soil amelioration with FGD gypsum" Resources, Conservation and Recycling Press.
World Health Organization. Handbook on indoor radon; 2009 [Geneva].
Yao Y. and Sun H. (2012). "A novel silica alumina-based backfill material composed of coal refuse and fly ash" *Journal of Hazardous Materials* 213, 71–82.
Ylmén R., Jäglid U., Steenari B. M. and Panas I. (2009). "Early hydration and setting of Portland cement monitored by IR, SEM and Vicat techniques" *Cement and Concrete Research* 39(5), 433–439.
Zhang N., Liu X., Sun H. and Li L. (2011). "Pozzolanic behaviour of compound-activated red mud-coal gangue mixture" *Cement and Concrete Research* 41, 270–278.
Zhang N., Li H. X., Zhao Y. Z. and Liu X. M. (2016). "Hydration characteristics and environmental friendly performance of a cementitious material composed of calcium silicate slag" *Journal of Hazardous Materials* 306, 67–76.